Catalysis Today 146 (2009) 279–284

Contents lists available at ScienceDirect

Catalysis Today

journal homepage: www.elsevier.com/locate/cattod

Electrochemical promotion of a platinum catalyst supported on the high-temperature proton conductor $La_{0.99}Sr_{0.01}NbO_{4-\delta}$

D. Poulidi [a,*], G.C. Mather [b], C.N. Tabacaru [b], A. Thursfield [a], I.S. Metcalfe [a]

[a] Department of Chemical Engineering and Advanced Materials, Newcastle University, NE1 7RU Newcastle upon Tyne, UK
[b] Instituto de Cerámica y Vidrio (CSIC), Cantoblanco, 28049 Madrid, Spain

ARTICLE INFO

Article history:
Available online 3 June 2009

Keywords:
Lanthanum niobate
Electrochemical promotion
Permanent promotion
Ceramic proton conductor
Impedance spectroscopy

ABSTRACT

The recently discovered, high-temperature proton conductor, $La_{0.99}Sr_{0.01}NbO_{4-\delta}$, was used as a support for the electrochemical promotion of a platinum catalyst. Ethylene oxidation was used as a probe reaction in the temperature range 350–450 °C. Moderate non-Faradaic rate modification, attributable to a protonic promoting species, occurred under negative polarisation; some permanent promotion was also observed. In oxidative atmospheres, both the p_{O_2} of the reaction mixture and the temperature influenced the type and magnitude of the observed rate modification. Rate-enhancement values of up to $\rho = 1.4$ and Faradaic-efficiency values approaching $\Lambda = -100$ were obtained. Promotion was observed under positive polarisation and relatively dry, oxygen-rich atmospheres suggesting that some oxygen ion conductivity may occur under these conditions. Impedance spectroscopy performed in atmospheres of 4 kPa O_2/N_2 and of 5 kPa H_2/N_2 under dry and slightly humidified (0.3 kPa H_2O) conditions indicated that the electrical resistivity is heavily dominated by the grain-boundary response in the temperature range of the EPOC studies; much lower grain-boundary impedances in the wetter conditions are likely to be attributable to proton transport.

© 2009 Elsevier B.V. All rights reserved.

1. Introduction

Electrochemical promotion of catalysis (EPOC), defined as the modification of the activity of a catalyst (mostly metallic) supported on an ionic conductor by the electrochemically induced spillover of promoting species onto the catalyst surface, is a phenomenon which has attracted much interest in the last 25 years [1].

Ethylene oxidation has been used as a model reaction in a variety of electrochemical promotion experiments using different catalysts and electrolytic membranes [1]. Several of these studies have been conducted using perovskite proton conductors such as, $CaIn_{0.9}Zr_{0.1}O_{3-\alpha}$ [2], $Ba_3Ca_{1.18}Nb_{1.82}O_{9-\alpha}$ [3] and $BaZr_{0.9}Y_{0.1}O_{3-\alpha}$ [4]. The promoting mechanism in the case of proton-conducting supports for ethylene oxidation on platinum has been studied by Thursfield et al. [3]. It is believed that under negative polarisation, protons from the electrolyte migrate onto the catalyst surface where they form surface hydroxyl groups via reaction with absorbed oxygen. The protons that are transported across the membrane can be replenished by water dissociation from the oxidation reaction products.

Here, we use $La_{0.99}Sr_{0.01}NbO_{4-\delta}$, a non-perovskite, high-temperature proton conductor, which adopts the fergusonite-type structure [5,6] below 500 °C, for the electrochemical promotion of ethylene oxidation. The $LaNbO_4$ system is of interest for exhibiting moderately high proton conductivity and better stability than its perovskite analogues, which tend to be reactive in acidic gases (e.g. CO_2) due to their high alkaline-earth-metal content.

2. Materials and methods

$La_{0.99}Sr_{0.01}NbO_{4-\delta}$ was prepared by solid-state reaction from dried precursors of La_2O_3 (99.98% purity), Nb_2O_5 (99.9%) and $SrCO_3$ (99.9%) in the appropriate stoichiometric ratios. The reagents were ground manually in an agate mortar and fired at 1100 °C for 12 h to allow decarbonisation to occur. The reactant mixture was then fired at 1250 °C for 24 h with intermediate grinding, subsequently ball-milled for 2 h in isopropyl alcohol, dried and sieved. Pellets of 20 mm diameter were pressed uniaxially from the sieved powder and sintered at 1500 °C for 6 h. Heating and cooling rates for all thermal treatments were 5 °C min^{-1}. Completeness of reaction and phase purity were confirmed by power X-ray diffraction (XRD) on ground pellets using a Siemens D5000 diffractometer with Cu Kα radiation. The density of the pellets was estimated using the Archimedes method. The microstructure of a fractured pellet and Pt catalyst morphology was analysed with a Zeiss DSM400 electron microscope.

Sintered pellets of $La_{0.99}Sr_{0.01}NbO_{4-\delta}$ were used in a single-chamber reactor for the electrochemical promotion of a platinum

* Corresponding author. Tel.: +44 191 2225747.
E-mail address: danai.poulidi@ncl.ac.uk (D. Poulidi).

0920-5861/$ – see front matter © 2009 Elsevier B.V. All rights reserved.
doi:10.1016/j.cattod.2009.04.025

catalyst during ethylene oxidation. A platinum film of a geometric projected area of 1 cm^2, which served as the catalyst and working electrode, was deposited onto one side of the pellet, and two gold films serving as the counter and reference electrodes were deposited on the opposing face. All metal electrodes were deposited by applying a coating of the respective metal paste followed by an appropriate drying and sintering regime. All experiments mentioned hereafter were conducted under atmospheric pressure (101.3 kPa).

The testing rig consisted of the gas-flow system, electrochemical reactor and furnace, gas analysis system and polarisation equipment. Gas flow was controlled via three Chell–Hastings electronic gas mass-flow controllers and gas analysis was performed by gas chromatography (Varian CP3800) and infrared spectroscopy (Binos 100 CO/CO_2 analyser). For the polarisation studies, an Amel 7050 potentiostat/galvanostat was used. The probe reaction was studied at temperatures of 350, 400 and 450 °C. Three pellets of thickness 1 mm (Pellet A) and 0.8 mm (Pellets B and C) were used. Different reaction mixtures were employed and both ethylene-rich and oxygen-rich conditions were used. Pellet A was used for initial exploratory experiments and as a comparison with Pellet B in terms of the effect of the electrolyte thickness. Pellet B was used under ethylene-rich conditions and Pellet C under oxygen-rich conditions. The reaction rates are expressed in terms of μmol cm^{-2} s^{-1} of atomic oxygen consumed according to the reaction: $C_2H_4 + 6O \rightarrow 2CO_2 + 2H_2O$, where the area used for the calculation is simply the geometric projected area of the catalyst film and not the actual surface area of the catalyst. For the polarisation experiments, a constant set of conditions was used throughout in order to obtain comparable results. Upon stabilisation of the open-circuit rate, the rate was monitored for 10 min and then the system was polarised for 60 min; on de-polarisation, the rate was monitored for a further 20 min (total experiment time, 90 min). Under some conditions, permanent EPOC was observed. In such cases the de-polarisation step was extended to 1000 min (i.e. the total experiment time was one order of magnitude longer). The OCV of the cell was approximately −120 mV and did not vary by more than 10 mV under different reaction mixture compositions.

Impedance spectroscopy was performed on a sintered pellet of $La_{0.99}Sr_{0.01}NbO_{4-\delta}$, which was first coated with Pt paste (SPi Supplies) on both faces and fired at 800 °C for 1 h to sinter electrodes. Data were collected with an Agilent 4294A instrument in the frequency range $40 \leq f \leq 10^7$ Hz, computer controlled with the Sweep software [7]. Measurements were taken in the range 350–550 °C on cooling in steps of 50 °C in dry atmospheres of 4 kPa O_2 and 5 kPa H_2, balance N_2 (L'Air Liquide, ≤3 ppm H_2O) and wetted atmospheres of similar compositions (0.3 kPa H_2O). The supplied gases were fed through drying or humidifying columns to a single-chamber furnace at a total set flow rate of 50 ml min^{-1}. A series of Bronkhorst mass flow controllers was employed to achieve the desired compositions, which were chosen in order to approximate the electrical behaviour of $La_{0.99}Sr_{0.01}NbO_{4-\delta}$ in the oxidising and reducing conditions employed in the EPOC experiments. The impedance spectra were resolved into bulk and grain-boundary contributions using the ZView software.

3. Results and discussion

3.1. Material characterisation

The powder X-ray diffraction pattern of the title-phase, sintered at 1500 °C (Fig. 1), showed the formation of X-ray phase-pure, fergusonite-type $LaNbO_4$ with monoclinic symmetry. Above 530 °C, a phase change to the high-temperature, tetragonal form of $LaNbO_4$ with the scheelite structure takes place. This phase

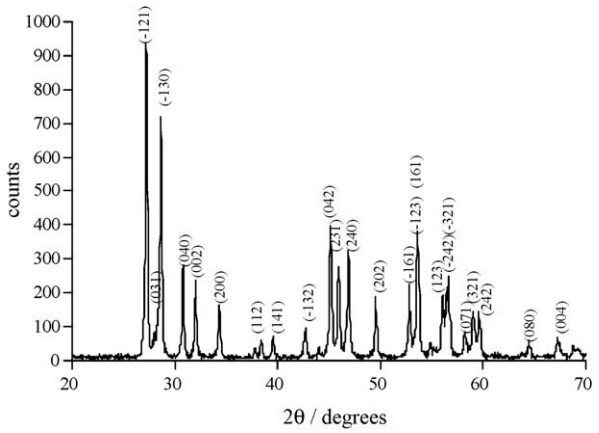

Fig. 1. X-ray powder diffraction pattern of $La_{0.99}Sr_{0.01}NbO_{4-\delta}$ with indexing of selected reflections (space group $I2/a$).

transition is associated with a break in conductivity to a lower activation-energy regime [5]. No EPOC experiments were conducted above the phase-transition temperature due to the limitation of electrochemical promotion at high temperature resulting from the destabilisation of the spillover species which form on the catalyst surface.

A secondary-electron scanning electron micrograph of a fracture surface of the $La_{0.99}Sr_{0.01}NbO_{4-\delta}$ membrane post operation, Fig. 2a, shows a grain size of 1–2 μm with no apparent open porosity. The densities of the membranes were >∼93% of the theoretical density. Similar densities have been reported for Sr-doped $LaNbO_4$ prepared from powder obtained by spray pyrolysis, with an equivalent final-firing regime [8]; in the latter case, grain size was slightly larger (3.6 μm for 2% doped Sr). A top view of the Pt catalyst, shown in Fig. 2b, reveals a particle size in the submicron range.

3.2. Potentiostatic transients

Pellet A was used in a series of preliminary experiments that were performed in order to determine the general behaviour of the novel support under EPOC conditions for ethylene oxidation. Solid-state cyclic voltammetry under reaction conditions was used in order to determine the profile of the promotion under a range of overpotentials. In Fig. 3, we can see the reaction rate transient during cyclic voltammetry performed between $\eta = -1$ and 1 V at a scan rate of 5 mV s^{-1}, the corresponding current response is also shown as an insert in Fig. 3. It can be seen that the reaction shows inverted volcano behaviour with respect to the applied overpotential. The current density as a function of the applied overpotential is also shown as an insert in Fig. 3. As we can see, the current density response is fairly featureless with no hysteresis between the anodic and cathodic polarisation steps. In contrast, the reaction-rate response to the overpotential sweep clearly shows some hysteresis during the return step (i.e. towards the open circuit potential) both under anodic and cathodic polarisation. This behaviour may be a result of slower kinetics for the formation (and dissociation) of the protonic species double layer on the catalyst surface when compared to the Faradaic charge transfer across the membrane.

Another observation we can make from Fig. 3 is that the rate modification under the studied conditions becomes more pronounced for positive polarisation, when protons are pumped away from the catalyst surface. This behaviour is in contrast with that of other materials that are predominantly proton conductors [2,3], where it has been found that negative polarisation promotes the reaction, whereas in general, positive polarisation has little or no

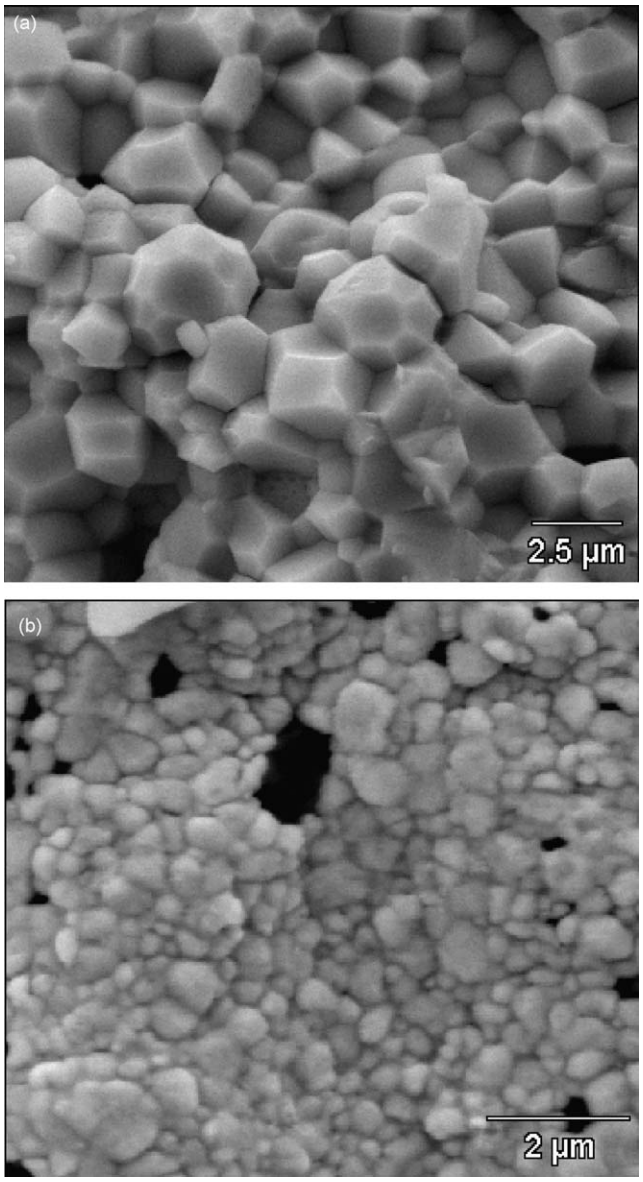

Fig. 2. Scanning electron micrographs of (a) transversal fracture surface of $La_{0.99}Sr_{0.01}NbO_{4-\delta}$ membrane and (b) top view of Pt catalyst surface.

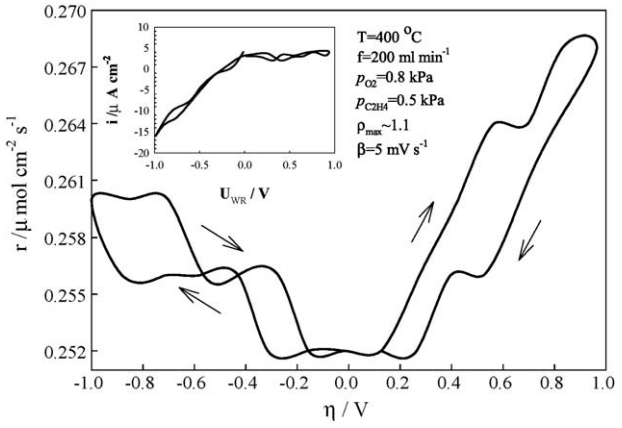

Fig. 3. Reaction rate transient on cyclic voltammetry at 400 °C, the insert figure shows the current density response to the applied overpotential.

effect. It has been determined that in the acceptor-doped $LaNbO_4$, proton conduction is the dominant transport mechanism in wet, reducing atmospheres [5], although a small oxide-ionic contribution to transport is observed which increases dramatically with temperature. It may be the case that in the dry, and relatively oxidising, conditions adopted here, oxide-ion conductivity is more significant since fewer oxygen vacancies will be protonated. This rate enhancement under positive polarisation in relatively dry conditions may, thus, be attributable to some oxide-ion species on the Pt surface. Similar behaviour has been observed previously in electrochemical promotion of ethylene oxidation using the mixed proton and oxide-ion conductor $BaZr_{0.9}Y_{0.1}O_{3-\delta}$ [9].

Fig. 4a shows a reaction-rate transient of Pellet B at 450 °C on applying an overpotential of −1 V, recorded under reducing conditions ($p_{C_2H_4} = 1.7$ kPa and $p_{O_2} = 0.4$ kPa). The corresponding maximum current density is also shown on the right-hand *y*-axis of Fig. 4a. It is apparent that, upon polarisation, the reaction rate increases rapidly from 0.38 to 0.43 μmol cm^{-2} s^{-1}. This fast increase is followed by a more gradual rate increase to a value of 0.48 μmol cm^{-2} s^{-1} within 1 h of polarisation. Upon returning to open-circuit conditions, the rate gradually drops after 20 min to a steady value of 0.42 μmol cm^{-2} s^{-1}, characteristic of permanent electrochemical promotion [10]. The measured maximum rate enhancement ratio was $\rho = 1.23$ with a Faradaic efficiency of $\Lambda = -7$, indicating a modest non-Faradaic behaviour (note that $\Lambda = \Delta r/(i/F)$ for a proton conductor [2,3], where Δr is the difference between the polarised and open-circuit rates, i is the current

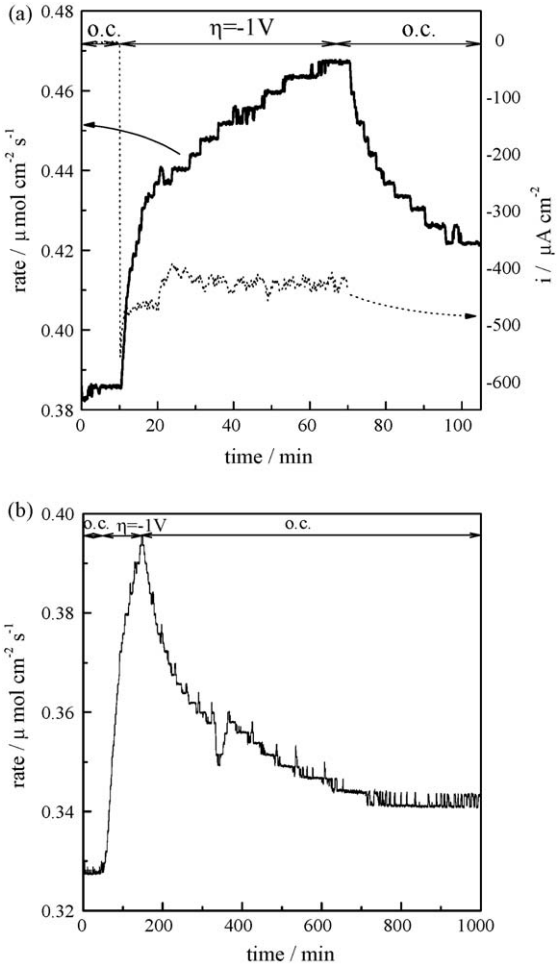

Fig. 4. (a) Reaction rate transient for Pellet B at 450 °C for $p_{C_2H_4} = 1.7$ kPa and $p_{O_2} = 0.4$ kPa, (b) long term reaction rate transient for Pellet C at 450 °C for $p_{C_2H_4} = 0.6$ kPa and $p_{O_2} = 2$ kPa exhibiting permanent promotion behaviour.

density and F is Faraday's constant). It is important to note that rate enhancement may be more significant on polarising for a longer period of time. Similarly, the permanent promotion may be less pronounced if the rate is monitored for longer upon return to open-circuit conditions.

Fig. 4b shows a rate transient obtained for Pellet C under an overpotential of −1 V at 400 °C under more oxidising conditions ($p_{C_2H_4} = 0.6$ kPa and $p_{O_2} = 2$ kPa). The maximum current density in this case (not shown here) was approximately −100 μA cm^{-2}. We can see that, again, some permanent promotion is observed. In this case the rate was monitored for a long period of time in order to monitor the slow return of the reaction rate to the initial open-circuit value. A maximum rate enhancement ratio of 1.4 is measured under these conditions. The Faradaic efficiency is the same as the transient shown in Fig. 4a at $\Lambda = -7$, indicating a weak non-Faradaic effect. As we can see from Fig. 4b, the reversibility of the observed promotion is very slow, taking more than 1000 min for the rate to drop to below an enhancement of around 5% (i.e. approximately 25% of the total observed promotion). Similar behaviour has also been observed for other proton-conducting supports such as the $Ba_3Ca_{1.18}Nb_{1.82}O_{9-\alpha}$ proton conductor [3].

3.3. Steady state kinetic experiments

Pellets A and B were used for measurement of the reaction kinetics as a function of the ethylene partial pressure, as shown in Fig. 5a. For Pellet A (1 mm thick), data exist only for 450 °C; for Pellet B (0.8 mm thickness), data were recorded at 350 and 450 °C. Pellet C (0.8 mm thickness) was used to record reaction kinetics with respect to the oxygen partial pressure of the reaction mixture, shown in Fig. 6. The inserts in Figs. 5a and 6a show the calculated rate-enhancement ratios and Figs. 5b and 6b the corresponding Faradaic-efficiency. Discrepancies between the reaction rates of the three pellets may arise as a result of irreproducibility of the precise area of Pt electrode coverage, electrode microstructure and the respective triple-phase-boundary lengths.

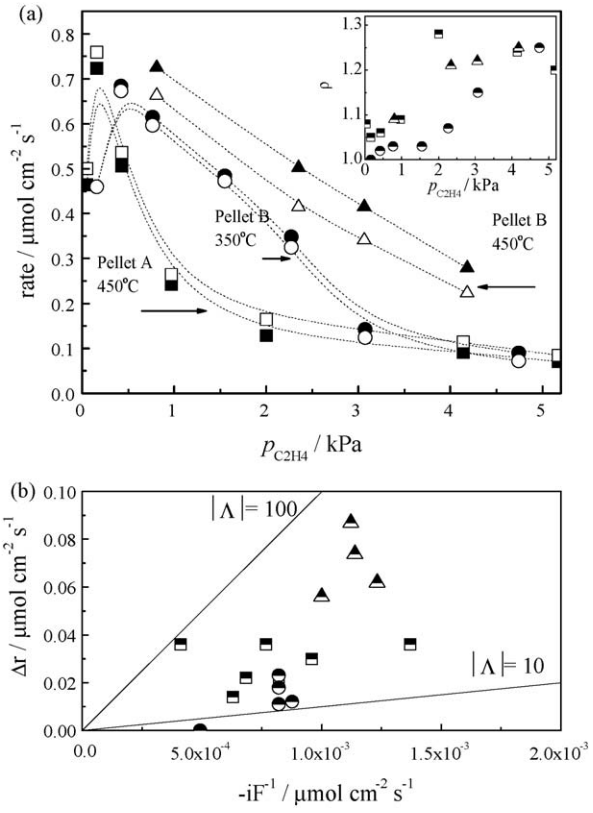

Fig. 5. (a) Reaction kinetics as a function of $p_{C_2H_4}$ for Pellets A and B. (b) Λ values for Pellets A and B.
For both pellets the flow rate was 360 ml (STP) min^{-1}. For Pellet A $p_{O_2} = 0.8$ kPa and for Pellet B $p_{O_2} = 0.4$ kPa. The measured current densities during the polarisation experiments were approximately −30 μA cm^{-2} for Pellet A at 450 °C and Pellet B at 350 °C and −400 μA cm^{-2} for Pellet B at 450 °C. In Fig. 2b and c, the symbols are assigned as follows: (□) Pellet A 450 °C, (○) Pellet B 350 °C, (△) Pellet B 450 °C, open symbols correspond to o.c. and filled symbols to polarised reaction rates. Half-filled symbols denote calculated parameters (i.e. ρ and Λ).

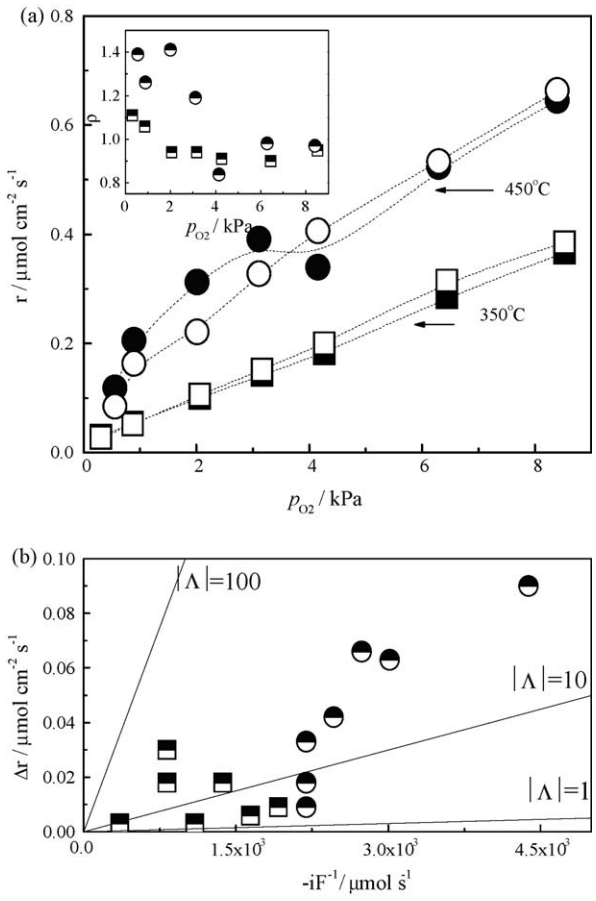

Fig. 6. (a) Reaction kinetics as a function of p_{O_2} for Pellet C. (b) Corresponding Λ values for Pellet C $f = 360$ ml (STP) min^{-1}, $p_{C_2H_4} = 0.6$ kPa, $i = -30$ μA cm^{-2} at 350 °C and $i = -100$ μA cm^{-2} at 450 °C. In Fig. 2b and c, the symbols are assigned as follows: (□) 350 °C, (○) 450 °C open symbols correspond to o.c. and filled symbols to polarised reaction rates. Half-filled symbols denote calculated parameters (i.e. ρ and Λ).

As can be seen from Fig. 5a, under a constant (low) oxygen partial pressure, negative polarisation has a moderate, non-Faradaic effect on the reaction rate for both Pellets A and B. A maximum rate enhancement ratio $\rho_{max} = 1.4$ is obtained and, as shown in Fig. 5b, Λ approaches values of −100 for both pellets. The behaviour of the two pellets is comparable.

In Fig. 6a, the reaction kinetics under a constant ethylene partial pressure are shown for oxygen partial pressures in the range 0.5–8.5 kPa, measured under open-circuit and polarised conditions using an overpotential of $\eta = -1$ V. It can be seen that, in contrast to the behaviour shown in Fig. 5 (under ethylene-rich conditions), both the temperature and the composition of the reaction mixture play a significant role in both the type (increase or decrease of the catalytic activity) of the observed rate modification and its magnitude. At 350 °C, a minor rate modification is observed and the effect is in fact Faradaic for low oxygen partial pressures, as demonstrated by the Λ values shown in Fig. 6b. Moreover, the applied overpotential appears to have an adverse effect on the

reaction rate for oxygen partial pressures higher than approximately 2 kPa, and the observed rate modification increases at higher partial pressure, reaching a rate-enhancement ratio of 0.84 at $p_{O_2} = 4$ kPa. At 450 °C, we observe a shift of the oxygen partial pressure threshold between promotion and poisoning of the catalytic activity from 2 kPa to approximately 4 kPa. Moreover, the observed promotion becomes more pronounced in the lower oxygen-partial-pressure range. It is interesting to note that the maximum rate-enhancement ratio is again observed at a $p_{O_2} =$ 4 kPa, only this time the rate modification is positive. In addition, the measurements conducted at 450 °C, where a rate enhancement was observed (i.e. for $p_{O_2} < 4$ kPa), were all characterised by permanent promotion, with a permanent enhancement ratio γ ~1.05. In cases where polarisation resulted in a rate decrease, no permanent promotion was observed. We must note, of course, that due to the small rate changes observed under these conditions, it is possible that some permanent modification did, in fact, occur but was not detectable due to experimental limitations.

The kinetic experiments conducted on the three pellets have shown that the reaction shows electrophilic behaviour under open-circuit conditions, with a positive rate order with respect to oxygen and negative order with respect to ethylene. According to the rules of electrochemical promotion [1], this suggests that oxygen (electron acceptor) is more weakly adsorbed than ethylene (electron donor) on the catalyst surface. Such behaviour has previously been reported using other proton-conducting supports for a platinum catalyst for ethylene oxidation [3,4,9]. This also suggests that, by applying a negative potential, in order to push protons onto the catalyst surface and decrease the catalyst work function, we should observe an increase of the catalytic activity. This scenario is confirmed experimentally for high ethylene-to-oxygen ratios. Such behaviour cannot always be observed for high oxygen partial pressures. It is possible that this is due to the presence of some oxygen-ion conductivity. This observation is consistent with both the cyclic voltammetry measurements discussed earlier and studies on the promotion of ethylene oxidation on a YSZ-supported platinum catalyst, where it has been consistently shown that positive polarisation (i.e. supply of oxygen ions to the catalyst) results in an increase of the reaction rate (e.g. refs. [11,12]).

3.4. Impedance spectroscopy

Impedance spectroscopy measurements were performed in order to investigate the conductivity of the material further and understand in more detail the promotional behaviour of the system. The impedance spectra were recorded under reducing ($p_{H_2} = 5$ kPa) and oxidising ($p_{O_2} = 4$ kPa) conditions both under dry (less than 3 ppm water) and humidified ($p_{H_2O} \sim 0.3$ kPa) atmospheres. Impedance spectra of $La_{0.99}Sr_{0.01}NbO_4$ in dry and humidified reducing conditions at 500 °C are shown in Fig. 7. The impedance data were modelled with an equivalent circuit consisting of two parallel RQ elements in series, $(R_1Q_1)(R_2Q_2)$, where R is the resistance, n is a constant-phase element and Q is the pseudo-capacitance related to the true capacitance through the relation

$$C = Q^{1/n}R^{1-n/n}$$

Capacitances of ~24 pF and 1.3 nF were determined for C_1 and C_2 in the water-containing reducing atmosphere at 500 °C (Fig. 7), typical of grain-bulk and grain-boundary responses, respectively. It can be seen in Fig. 7 that the impedance response is heavily dominated by the grain-boundary resistance, which is much larger still in the drier conditions in comparison to the wetter atmosphere similar to the ethylene-rich experimental conditions of the EPOC experiments. Similarly, the grain-boundary response was considerably less resistive in H_2O-containing oxidising conditions in comparison with the dry oxidising regime, although the magnitude of the change was less than that observed in reducing atmospheres. This indicates that proton transport is favoured in the grain boundaries in the presence of H_2O and that in dry conditions, where electronic charge carriers are likely to predominant, the grain boundaries are highly blocking. Total resistances at 500 °C were estimated to be ~2.7×10^{-4} and 5.0×10^{-5} S cm^{-1} in the H_2O-containing reducing and oxidising conditions, respectively. An Arrhenius plot of the deconvoluted bulk conductivities, shown in Fig. 8, indicates a somewhat lower resistance for $La_{0.99}Sr_{0.01}NbO_{4-\delta}$ in the H_2O-containing, reducing atmosphere in comparison to the other studied conditions (apparent activation energies for the deconvoluted bulk conductivities were in the range 1.08–1.29 eV) The transition to a lower activation activation-energy regime above 500 °C in the Arrhenius plot, associated with the phase transition to scheelite-type, tetragonal $LaNbO_4$, is apparent. We note that Haugsrud and Norby [6] have reported that the doped $LaNbO_4$-based system exhibits predominantly ionic transport over a wide p_{O_2} domain, in wetter conditions ($p_{H_2O} = 2.5$ kPa) and at higher temperatures, where conductivity is dominated by the bulk response.

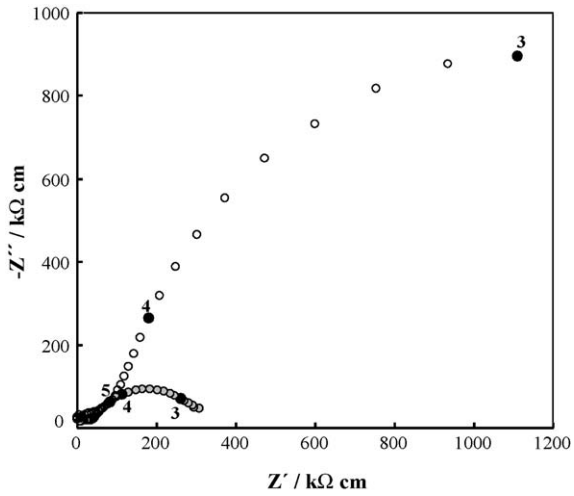

Fig. 7. Impedance spectra of $La_{0.99}Sr_{0.01}NbO_{4-\delta}$ at 550 °C in 5 kPa H_2 in N_2 for dry (open symbols) and H_2O-containing conditions (grey symbols, 0.02 kPa H_2O).

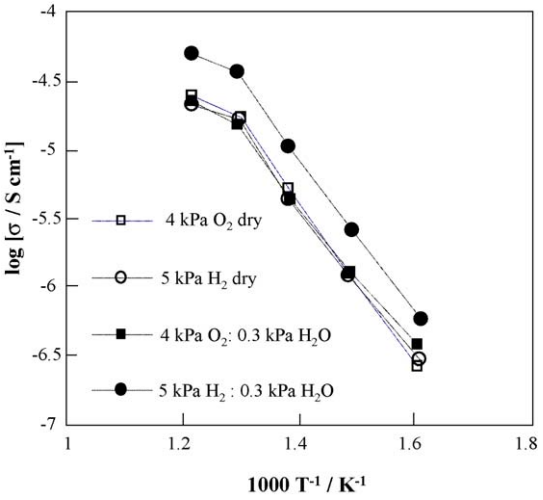

Fig. 8. Temperature dependence of the deconvoluted bulk conductivity of $La_{0.99}Sr_{0.01}NbO_{4-\delta}$ (balance of gases, N_2).

4. Conclusions

The recently discovered, high-temperature proton conductor, $La_{0.99}Sr_{0.01}NbO_{4-\delta}$, was used as a support for a platinum catalyst in the electrochemical promotion of ethylene oxidation under high oxygen partial pressures. The reaction showed inverted volcano behaviour, with a more pronounced effect observed for positive overpotentials, which may originate from some oxide-ion conductivity in dry, mildly oxidising conditions. Under ethylene-rich conditions moderate promotion was observed under negative polarisation, where proton conductivity is expected to dominate transport, suggesting that a moderate non-Faradaic process takes place. Under oxygen-rich conditions, both the temperature and the reaction-mixture composition affected the rate modification. At high oxygen partial pressures, a rate decrease was observed under polarisation, while for higher temperatures, the threshold between promotion and poisoning of the catalyst was shifted to lower p_{O_2}. Permanent promotion was also observed in some cases for both ethylene- and oxygen-rich reaction mixtures. To the best of our knowledge, the study is the first to demonstrate electrochemical promotion with a non-perovskite, proton-conducting ceramic support. The $LaNbO_4$-based phase is of particular interest as an electrochemical reactor due to its higher expected stability in acidic atmospheres, such as CO_2, in comparison with other high-temperature, proton-conducting oxides.

Acknowledgments

The authors would like to thank the Royal Society for funding this work via the International Joint Project scheme (grant number JP071195). ISM acknowledges the financial support of the Centre for Process Innovation, Wilton, UK and DP the Engineering and Physical Sciences Research Council (grant number EP/E033687/1).

References

[1] C.G. Vayenas, S. Brosda, C. Pliangos, Journal of Catalysis 203 (2001) 329.
[2] M. Makri, A. Buekenhoudt, J. Luyten, C. Vayenas, Ionics 2 (1996) 282.
[3] A. Thursfield, S. Brosda, C. Pliangos, T. Schober, C.G. Vayenas, Electrochimica Acta 48 (2003) 3779.
[4] D. Poulidi, M.A. Castillo-del-Rio, R. Salar, A. Thursfield, I.S. Metcalfe, Solid State Ionics 162–163 (2003) 305.
[5] R. Haugsrud, T. Norby, Solid State Ionics 177 (2006) 1129.
[6] R. Haugsrud, T. Norby, Nature Materials 5 (2006) 193.
[7] J.C.C. Abrantes, J.R. Frade, ISA – Impedance Spectroscopy Analysis, Software Package ESTG/IPVC, 2003.
[8] T. Mokkelbost, Ø. Andersen, R.A. Strøm, K. Wiik, T. Grande, M.-A. Einarsrud, Journal of the American Ceramic Society 90 (2007) 3395.
[9] D. Poulidi, I.S. Metcalfe, Solid State Ionics 177 (2006) 2211.
[10] C. Falgairette, A. Jaccoud, G. Fóti, C. Comninellis, Journal of Applied Electrochemistry 38 (2008) 1075.
[11] S. Bebelis, M. Makri, A. Buekenhoudt, J. Luyten, S. Brosda, P. Petrolekas, C. Pliangos, C.G. Vayenas, Solid State Ionics 129 (2000) 33.
[12] C. Koutsodontis, A. Katsaounis, J. Figueroa, C. Cavalca, C. Pereira, C. Vayenas, Topics in Catalysis 38 (2006) 157.